NANO LETTERS

2007
Vol. 7, No. 9
2800−2805

Fabrication of Large-Area Patterned Nanostructures for Optical Applications by Nanoskiving

Qiaobing Xu,[†] Jiming Bao,[‡] Robert M. Rioux,[†] Raquel Perez-Castillejos,[†] Federico Capasso,[‡] and George M. Whitesides*,[†]

Department of Chemistry and Chemical Biology, Harvard University, 12 Oxford Street, Cambridge, Massachusetts, 02138, and Harvard School of Engineering and Applied Sciences, Harvard University, 29 Oxford Street, Cambridge, Massachusetts, 02138

Received June 11, 2007

ABSTRACT

Cost-effective and convenient methods for fabrication of patterned metallic nanostructures over the large (mm^2) areas required for applications in photonics are much needed. In this paper, we demonstrate the fabrication of arrays of closed and open, loop-shaped nanostructures by a technique (nanoskiving) that combines thin-film deposition by metal evaporation with thin-film sectioning. These arrays of metallic structures serve as frequency-selective surfaces at mid-infrared wavelengths. Experiments with structures prepared using this technique demonstrate that a closed-looped structure has a single dominant resonance regardless of the polarization of the incident light, while open structures have resonances that are anisotropic with respect to the polarization of the electric field. Finite-difference time-domain (FDTD) simulations reproduce the scattering spectra of these frequency-selective surfaces, provide an explanation of the wavelength of the experimentally observed resonances, and rationalize their polarization dependence based on the patterns of current induced in the nanostructures.

This paper describes the fabrication by nanoskiving[1−3] of large-area (∼9 mm^2), thin (∼100 nm), free-standing epoxy slabs incorporating regular arrays of metallic nanostructures. We measured the transmission spectra of these nanostructures and compared them with simulated scattering spectra using finite-difference time-domain (FDTD) calculations. Experimentally, closed-loop structures have a single dominant resonance regardless of the polarization of the incident light. Open structures — e.g., L- or U-shaped structures — have resonances that are anisotropic with respect to the polarization of the electric field. The FDTD calculations adequately reproduce the spectra and provide a simple explanation for the wavelengths of resonances, and of their polarization dependence, based on the patterns of current induced in the nanostructures by the incident light. We believe that the ability to fabricate and manipulate free-standing metallic nanostructures will find applications in the fabrication of materials having negative index of refraction and of three-dimensional metamaterials.[4−10]

Patterned arrays of metallic nanostructures have wide applications in photonics, in (for example) negative index materials (NIMs),[4−10] frequency-selective surfaces (FSS),[11−20] optical polarizers, optical filters, and nanostructures for surface-enhanced Raman spectroscopy (SERS).[21,22] FSS are two-dimensional periodic arrays of metallic structures that transmit or reflect radiation at specific frequencies; FSS are useful in beam splitters, filters, and polarizers.[13−15] In FSS, the reflection or transmission is strongest when the frequency of the incident electromagnetic field matches the plasmon resonance of the metallic structures comprising the FSS. This resonant frequency is mainly determined by the size and shape of the unit metallic nanostructures comprising the FSS. The bandwidth of the resonance — as well as the total reflectivity or transmittance — depends on the density and periodicity of unit elements.[15] For a FSS consisting of identical, straight, metallic wires (an antenna array) of length l, the longest wavelength of resonance is approximated by eq 1, where λ_r is the resonance wavelength and n_{eff} is the effective refractive index of the medium.

$$\lambda_r/2 \sim n_{eff} l \tag{1}$$

$$n_{eff} = \left(\frac{n_1^2 + n_2^2}{2}\right)^{1/2} \tag{2}$$

In eq 2, n_1 and n_2 are refractive indices of the media above (air, $n = 1$) and below (supporting substrate) the metallic nanostructure.[15,23] At the resonant wavelength λ_r, the wire behaves approximately as a simple electric dipole. For simple

* Corresponding author. Telephone: (617) 495-9430. Fax: (617) 495-9857. E-mail: gwhitesides@gmwgroup.harvard.edu.
[†] Department of Chemistry and Chemical Biology.
[‡] Harvard School of Engineering and Applied Sciences.

10.1021/nl0713979 CCC: $37.00
Published on Web 08/01/2007

non-straight wires (for example, one having L or U shape), the dominant resonance is still approximately given by eq 1.[15] In addition to this long wavelength resonance, strong high-order resonances at shorter wavelength can also be excited at normal incidence with proper polarization of the incident light. We have observed these strong harmonics in L-shaped and U-shaped structures.

A FSS can also couple to incident light magnetically if it contains split-ring or U-shaped structures, because the oscillating magnetic field component of the incident light perpendicular to the plane of the nanostructures can induce an oscillating electrical current in them. U-shaped metallic structures with dimensions of 300 nm have a magnetic resonance at infrared wavelengths;[5,9,10] they can be used to construct NIMs (if they are co-assembled with thin-wire structures as composite nanostructures).[6]

For wavelengths in the mid-infrared (MIR) (4−20 μm), near-infrared (NIR) (0.8−4 μm), and the visible (0.8−0.4 μm) regions, the sizes of feature necessary for functional FSS are on the order of the wavelength of light (eq 1); for NIR/MIR FSS, these dimensions require either conventional photolithography or more complex techniques, such as extreme ultraviolet or X-ray lithography.[11−13,24] These techniques work well for the generation of test structures, but they are complex, expensive, not applicable to non-planar surfaces, and incompatible with many materials. Cost-effective and convenient methods for fabrication of patterned metallic nanostructures over the large (mm^2) areas required for applications in FSS and NIMs are much needed.[13,16−19,25−27] Nanoskiving is a useful technique for fabricating patterned nanoscale structures.[1−3] In this paper, we demonstrate the use of square posts as a template for the fabrication of arrays of closed and open, loop-shaped nanostructures over areas as large as ∼9 mm^2 and illustrate the function of these nanostructures as optical filters at mid-infrared frequencies.

Fabrication of Square Closed Loop-Shaped Nanostructures over a Large Area by Nanoskiving and Their Optical Properties. Figure 1 sketches the use of nanoskiving to fabricate closed-loop nanostructures.[3] (A "closed-loop" structure is one comprising a topologically continuous loop; an "open" structure is one that has two ends—that is, a closed-loop structure with one cut.) Here we modify the published procedure[2,3] to fabricate approximately square, open-loop gold nanostructures in arrays extending over areas up to ∼9 mm^2. Briefly, we fabricated epoxy substrates patterned with ∼2 × 2 μm square posts by casting epoxy prepolymer on a poly(dimethylsiloxane) (PDMS) mold (using standard soft-lithographic procedures) on a 15 nm thick film of gold supported on a test-grade silicon wafer with a thin layer of native SiO_2 (∼2 nm).[3] The gold layer facilitates separation of the epoxy from the Si/SiO_2 substrate: gold adheres poorly to Si/SiO_2 in the absence of an adhesion-promoting layer such as Ti or Cr. We deposited a 40 nm thick gold film isotropically on these square epoxy posts (or selectively on their sides and top) using line-of-sight or shadow (angle) deposition by electron-beam evaporation. Embedding the metal-coated epoxy substrate in more epoxy of the same kind generated an epoxy block containing the topographically

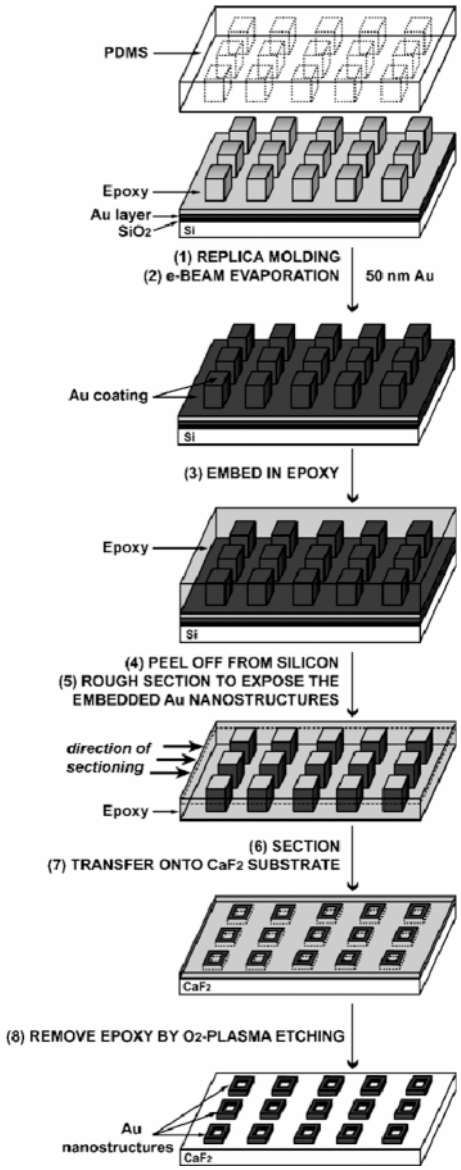

Figure 1. Schematic illustration of the procedure used to fabricate arrays of approximately square loop-shaped nanostructures on a solid substrate (e.g., CaF_2). Square structures are fabricated by isotropic coating of square posts with gold by electron-beam evaporation, followed by nanoskiving. Fabrication of L- and U-shaped nanostructures is accomplished starting with the same square posts and depositing Au by shadow evaporation.

structured thin gold film. We trimmed the epoxy substrate into a block with an area of 2 mm by 1.5 mm with a razor blade ("rough sectioning") and sectioned this block in a plane parallel to the patterned surface using an ultramicrotome (Leica UCT) equipped with a diamond knife (Diatome, 45° knife angle). The edge of the knife and face of the epoxy block must be carefully aligned in order to obtain slabs of uniform thickness over a large area (∼3 mm^2). Alignment requires several steps; a detailed procedure for microtome alignment is included in the Supporting Information.

We collected the epoxy slabs on the surface of the water contained in the sample trough mounted to the backside of the diamond knife. We transferred these thin epoxy sections onto a solid substrate (e.g., a TEM grid, or single-crystal CaF_2 or ZnSe) by submerging small sections of the substrate

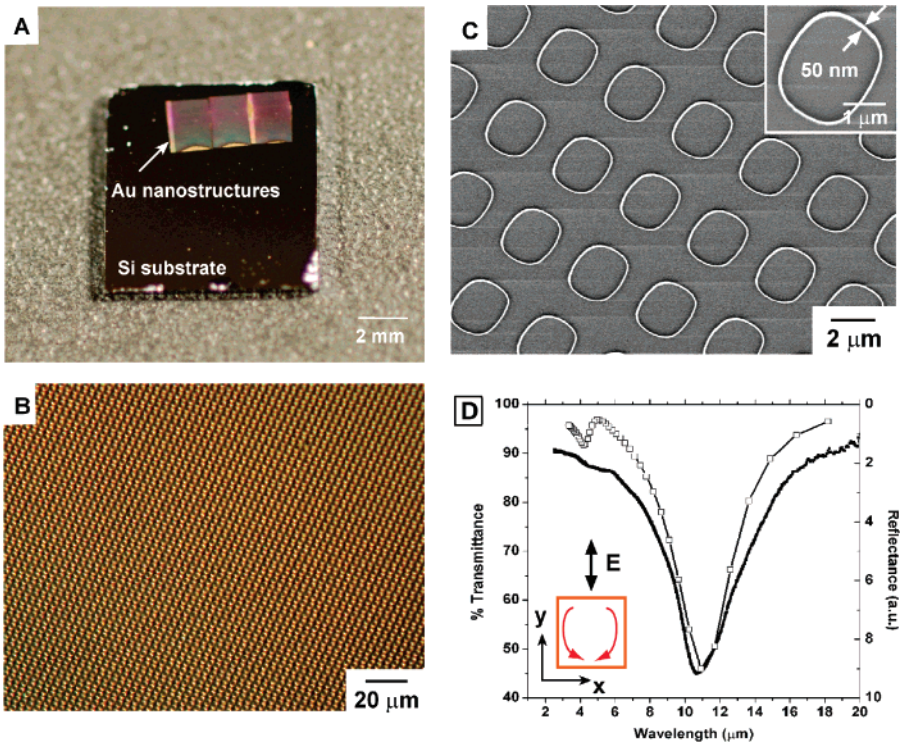

Figure 2. (A) Photograph of the patterned square loop-shaped nanostructure on a SiO_2/Si(100) substrate, after removal of the epoxy matrix with an oxygen plasma. (B) Dark-field optical microscopy image of the array of nanostructures. (C) SEM image of an array of 50 nm wide, 100 nm tall closed-loop gold nanostructure on a SiO_2/Si(100) substrate. (D) Infrared transmission spectrum (solid line) measured through an array of gold nanostructures supported on ZnSe; E is the direction of polarization of the light relative to the loop. FDTD simulation (open symbols) of the reflectance spectra through a single Au nanostructure assuming an effective dielectric constant of $n_{eff} = 1.8$ (eq 2).

in the trough, and pulling it toward the surface in a way that allowed the floating polymer film containing the gold nanostructures to settle on it. We removed the epoxy matrix by etching in an oxygen plasma; this process left the array of gold nanostructures supported on the solid substrate.

As the epoxy slabs are generated by the action of the diamond knife, they are transferred to the surface of the water. There, capillary forces cause them to form ordered aggregates; this self-assembly enables us to generate large-area patterns.[28] Figure 2A is a photograph of the square, closed-loop nanostructures on a silicon substrate patterned over a ~9 mm^2 area; this area reflects the self-assembly of three individual epoxy slabs (each 3 mm^2) into a rectangle. Figure 2B is the dark-field optical microscopy image of the square-loop nanostructures. The SEM images in Figure 2C show nanostructures with a wall thickness of ~50 nm and with 100 nm height. These two dimensions correspond to the thickness of the gold film deposited by e-beam evaporation and of the thickness of the epoxy slab generated by the microtome.

Figure 2D is the IR transmission spectrum of the square-loop nanostructures on a ZnSe substrate ($n_{eff} = 1.8$ with $n_{ZnSe} = 2.4$ at 11 μm and $n_{air} = 1$). We observed a single major resonant peak at 11 μm independent of the polarization of the incident infrared light, with a transmittance of 45% at the wavelength of maximum scattering. In previous FSS work

$$\lambda_r \approx n_{eff} C \qquad (3)$$

was used to estimate the resonant wavelength,[11,16−18] where C is the perimeter of the loop. This resonant condition can be explained by the following physical argument. For simplicity, we assume the incident light is polarized along the y-axis as shown in the inset of Figure 2D. The red arrows suggest the pattern of the induced electrical current. There are two oscillating currents with mirror symmetry and with the mirror plane parallel to the polarization of the electric field. In this geometry, the electric field induces two mirror dipoles, each with a length $l = C/2$. According to eq 1, the resonance wavelength for each of these is given by $\lambda_r \sim 2n_{eff}l = n_{eff}C$, which is consistent with the result from eq 3. Even when the polarization is not along the y-axis, each induced dipole still has length l equal to $C/2$; these orientations also result in the same resonance wavelength, ~11 μm. In any case, two dipoles are induced by the electrical field; each dipole involves half of the total length of the loop, which explains why we observe only a single resonance peak, whose position is independent of the polarization of the incident light. This argument is applicable to FSS made of simple closed structures.[11,16−18] Figure 2D (open symbols) is the calculated back scattering spectrum from a single square simulated using FDTD methods. The peak position and its resonance width derived from FDTD simulation are in good quantitative agreement with the data.

Fabrication of Open Nanostructures from Square Templates and Their Optical Properties. We fabricated open nanostructures by modifying the procedure for metal deposition. We used shadow evaporation from single or

multiple directions to coat two or three sides of the template of square epoxy posts selectively. A single shadow evaporation with the sample mounted 60° from the plane for line-of-sight evaporation onto a single corner or three consecutive shadow evaporations from three edges of the square template generated L-shaped and U-shaped nanostructures, respectively. Figure 1 is also a summary of this procedure, with the exception that it does not explicitly show the side-selective evaporations.

L-Shaped Nanostructure and Transmission Spectra. Figure 3A is the dark-field optical microscopy image of L-shaped nanostructures patterned over a ~3 mm^2 area. These nanostructures have a wall thickness of ~50 nm, and are 100 nm in height. Figure 3B is the transmission spectrum of an array of these L-shaped nanostructures supported on a CaF_2 substrate ($n_{eff} = 1.2$, with $n_{CaF_2} = 1.36$ at 7 μm, and $n_{air} = 1$). The spectrum exhibits two dominant transmission band-stops in the mid-infrared region (respectively) centered at 8.4 and 4.8 μm, with maximum transmissions of 67% and 82%. The L-shaped structure is less isotropic than a square structure with respect to the polarized incident light. In order to study the polarization dependence of both resonances, we used linearly polarized light by inserting a broadband wire polarizer in the path of the incident beam. The 8.4 μm long wavelength resonance is observed when the polarization of incident light is parallel to a line connecting the two ends of the L-structure (Figure 3C). Figure 3D shows a single resonant peak at 4.8 μm obtained with the polarization perpendicular to the line connecting the two ends of the L.

There are two different patterns of electrical current in the L-shaped structure responsible for the resonances shown in parts C and D of Figure 3. The inset of Figure 3C shows the first current pattern (fundamental mode, half-wavelength resonance) oscillating between the two tips of the L when the E field points from one tip of the L to the other tip. In this case, l in eq 1 is the sum of the lengths of both arms of the L-shaped nanostructure. This current distribution is responsible for the 8.4 μm resonance. When the polarization of the incident light is perpendicular to the line connecting the two ends of the L (Figure 3D), a relatively symmetric current pattern is induced, in which the L is effectively split into two antennae (two dipoles) oscillating in phase. The length for each dipole is about half of the total length. This current is responsible for the 4.8 μm resonance: it is a harmonic mode of the 8.4 μm mode. With this polarization, only the 4.8 μm mode is excited, and the fundamental mode at 8.4 μm is suppressed. At other polarizations, both modes will be excited (see Supporting Information Figure 1 for polarization parallel to the two perpendicular arms). Due to the near-field electrostatic interaction between two harmonic dipoles, the actual resonant wavelength (4.8 μm) is not exactly at half of the fundamental wavelength (8.4 μm). FDTD simulations of the back scattering spectra at both polarization conditions in parts C and D of Figure 3 (open symbols) demonstrate that the calculated resonance position and bandwidth agree with experimental measurements.

U-Shaped Nanostructure and Transmission Spectra. A U-shaped structure is a simplified version of the split-C

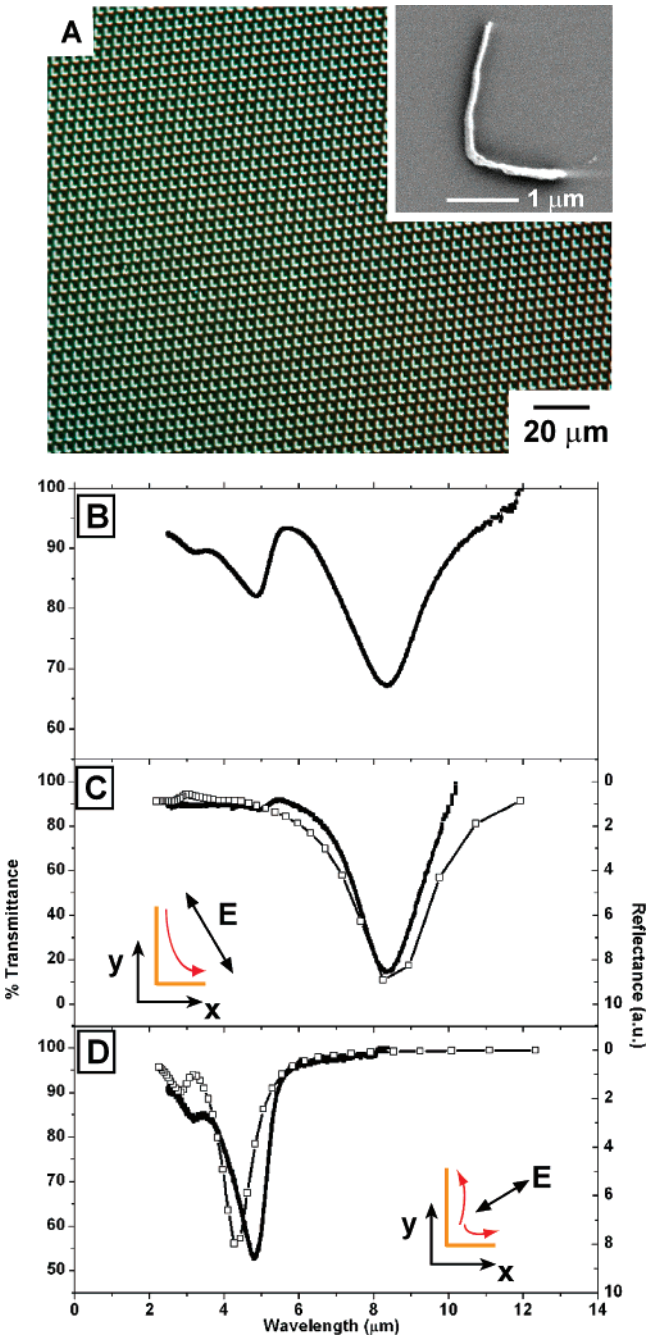

Figure 3. (A) Dark-field optical image of L-shaped gold nanostructures on a CaF_2 substrate, after removal of the epoxy matrix with an oxygen plasma. The inset is the SEM image of a 50-nm wide, 100-nm tall L-shaped gold nanostructure. (B) IR transmission spectrum (solid line) of an array of L-shaped gold nanostructures supported on CaF_2. (C, D) The transmission spectra of L-shaped nanostructure with incident light polarization parallel (C) or perpendicular (D) to the line connecting the two ends of the L-structure. The inset diagram illustrates the polarization direction (black arrow) and induced current flow (red arrow) in the L-shaped nanostructure (orange) for two polarizations of the incident light. FDTD simulation (open symbols) of the reflectance spectra through a single Au nanostructure unit on CaF_2 substrate assuming an effective dielectric constant of $n_{eff} = 1.2$ (eq 2).

structure proposed by Pendry for the construction of materials with negative index of refraction.[7,8] We fabricated U-shaped nanostructures by nanoskiving by coating three sides of the

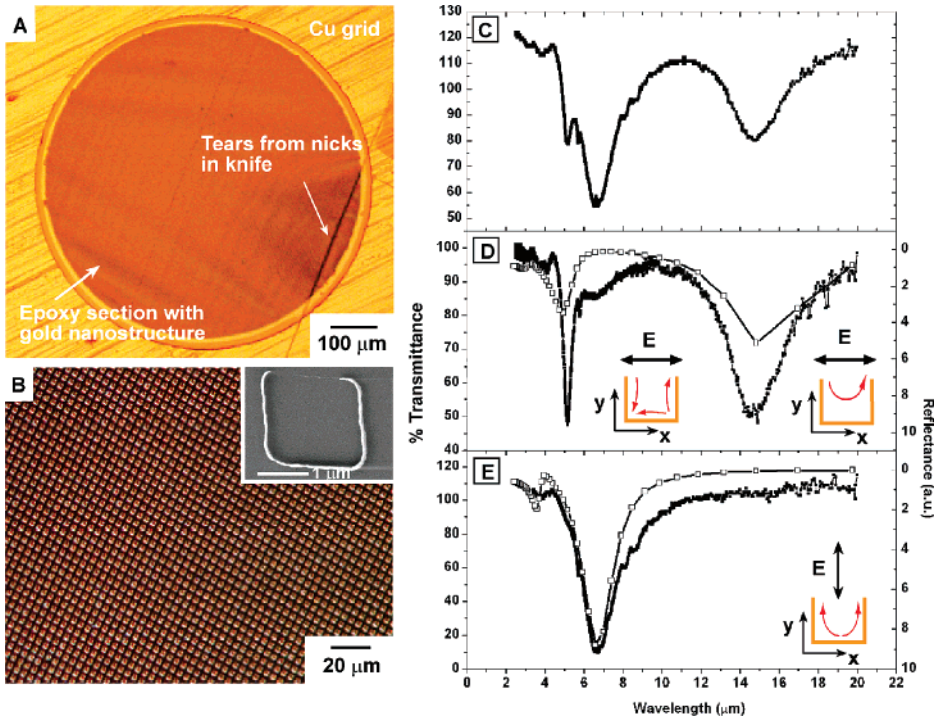

Figure 4. (A) Bright-field optical image of an epoxy slab containing U-shaped nanostructures sitting on top of a hole in a copper sheet. (B) Dark-field optical image of the array of U-shaped nanostructures. The inset is a high-magnification SEM image of a single U-shaped nanostructure with a wall thickness of ~50 nm, and 100 nm height. (C) Transmission spectrum of the epoxy-embedded array of U-shaped nanostructures, suspended over a hole, using unpolarized incident light. (D, E) Transmission spectra of U-shaped structures with the polarization of the incident light parallel (D) or perpendicular (E) to the line connecting the two ends of the U. The inset relates the direction of polarization (black arrow) and the induced current (red arrows) in the U-shaped nanostructure (orange) for different polarizations of the incident light. FDTD simulation (open symbols) of the reflectance spectra through a single Au nanostructure unit embedded in epoxy assuming an effective dielectric constant of $n_{eff} = 1.2$ for the epoxy.

template of square epoxy posts. Equation 1 indicates that we should observe the fundamental mode (longest wavelength resonance) at $\lambda > 10$ μm when l is defined as the total length of U (~6 μm because each side of the square is 2 μm). CaF_2 substrate is not transparent at wavelengths above ~10 μm and is not a suitable substrate for transmission characterization of U-shaped nanostructure with a total length ~6 μm.

The ability to manipulate the free-standing epoxy slab containing the array of U-shaped nanostructure allows us to measure the optical properties of this array without a supporting substrate (but with the nanostructure remaining embedded in the epoxy film). Figure 4A is an optical image of a thin epoxy section (100 nm) containing U-shaped nanostructures suspended over a hole (~700 μm diameter) in a copper sheet (~300 μm thick). Figure 4B is an enlarged dark-field optical image of the U-shaped nanostructure in the epoxy matrix. The inset is a high-magnification SEM image of a single U-shaped nanostructure with a wall thickness of ~50 nm, and 100 nm height. The shape of the nanostructures showed some deformation relative to that of the original template, which is attributed to the compression that the knife exerts on the sample during sectioning.[3] We measured the transmission spectra of this sample directly using a piece of epoxy film having the same thickness as a reference (see Supporting Information Figure 2). We observed three distinct resonant peaks from this sample in the mid-IR region at 5.1, 6.5, and 14.5 μm, respectively (Figure 4C).

The U-shaped structure is not isotropic with respect to the polarization of incident light, and the observed number and wavelength of the resonance are dependent on the polarization of the incident light. The right inset of Figure 4D suggests the resonant current for the given polarization. In this pattern, the induced current oscillates between the ends of the U-shaped nanostructure. The left inset of Figure 4D is the current pattern responsible for the harmonic mode. There are three dipole oscillators excited along the wire. The length of each oscillator is about a third of the total length; the corresponding resonant frequency is approximately three times higher than the resonant frequency of the fundamental dipole mode (i.e., a half-wavelength resonance). The inset of Figure 4E shows the current pattern when the E-field of the light is perpendicular to the open side. In this case, two symmetric dipoles are induced, and the corresponding length is half of the total length for each dipole.

In conclusion, nanoskiving provides an effective new method to make dense, large-area (9 mm^2 by assembling three slabs as shown in Figure 2A), highly ordered arrays of nanostructures. These structures have the right dimensions required to test many of the properties of nanostructures acting as true plasmonic oscillators in the IR (and, we believe, visible) regions of the electromagnetic spectrum. Here we demonstrate the ability of arrays of L- and U-shaped

nanostructures to serve as mid-infrared band-stop optical filters. We used a simple formula (eq 1) to estimate the resonance wavelength related to the geometry of the nanostructure and determined the length of the induced currents in these nanostructures by FDTD simulations in order to generate fundamental and higher order harmonic resonances. The U-shaped structure is a simplified version of a split-C oscillator —a structure with useful characteristics as an RC circuit element operating in the optical region and relevant to metamaterials.[4−10]

Acknowledgment. This research was supported by NIH (GM065364), a DARPA subaward to G.M.W. from the Center for Optofluidic Integration at the California Institute of Technology, and by a MURI AFOSR on Plasmonics subaward to F.C. This work was performed in part at the Center for Nanoscale Systems (CNS), a member of the National Nanotechnology Infrastructure Network (NNIN), which is supported by the National Science Foundation under NSF award no. ECS-0335765. CNS is part of the Faculty of Arts and Sciences at Harvard University. R.M.R. acknowledges the support of NIH in the form of a postdoctoral fellowship (1 F32 NS060356). R.P.-C. acknowledges the support of MRSEC in the form of a postdoctoral fellowship. J. M. Bao thanks Ertugrul Cubukcu for many valuable discussions.

Supporting Information Available: Detail of the nanofabrication process and the optical characterization. This material is available free of charge via the Internet at http://pubs.acs.org.

References

(1) Xu, Q.; Gates, B. D.; Whitesides, G. M. *J. Am. Chem. Soc*. **2004**, *126*, 1332−1333.
(2) Xu, Q.; Bao, J. M.; Capasso, F.; Whitesides, G. M. *Angew. Chem., Int. Ed*. **2006**, *45*, 3631−3635.
(3) Xu, Q.; Perez-Castillejos, R.; Li, Z. F.; Whitesides, G. M. *Nano Lett*. **2006**, *6*, 2163−2165.
(4) Yen, T. J.; Padilla, W. J.; Fang, N.; Vier, D. C.; Smith, D. R.; Pendry, J. B.; Basov, D. N.; Zhang, X. *Science* **2004**, *303*, 1494−1496.
(5) Soukoulis, C. M.; Kafesaki, M.; Economou, E. N. *Adv. Mater*. **2006**, *18*, 1941−1952.
(6) Shelby, R. A.; Smith, D. R.; Schultz, S. *Science* **2001**, *292*, 77−79.
(7) Pendry, J. B.; Holden, A. J.; Robbins, D. J.; Stewart, W. J. *IEEE Trans. Microwave Theory Technol*. **1999**, *47*, 2075−2084.
(8) Pendry, J. B. *Phys. Rev. Lett*. **2000**, *85*, 3966−3969.
(9) Linden, S.; Enkrich, C.; Wegener, M.; Zhou, J. F.; Koschny, T.; Soukoulis, C. M. *Science* **2004**, *306*, 1351−1353.
(10) Enkrich, C.; Wegener, M.; Linden, S.; Burger, S.; Zschiedrich, L.; Schmidt, F.; Zhou, J. F.; Koschny, T.; Soukoulis, C. M. *Phys. Rev. Lett*. **2005**, *95*, 203901.
(11) Kogler, K. J.; Pastor, R. G. *Appl. Opt*. **1988**, *27*, 18−19.
(12) Krug, P. A.; Dawes, D. H.; McPhedran, R. C.; Wright, W.; Macfarlane, J. C.; Whitbourn, L. B. *Opt. Lett*. **1989**, *14*, 931−933.
(13) Morgan, M. D.; Horne, W. E.; Sundaram, V.; Wolfe, J. C.; Pendharkar, S. V.; Tiberio, R. *J. Vac. Sci. Technol., B* **1996**, *14*, 3903−3906.
(14) Wu, T. K. *Microwave Opt. Technol. Lett*. **1997**, *15*, 9−12.
(15) Munk, B. A. *Frequency selective surfaces: theory and design*; Wiley: New York, 2000.
(16) Paul, K. E.; Zhu, C.; Love, J. C.; Whitesides, G. M. *Appl. Opt*. **2001**, *40*, 4557−4561.
(17) Love, J. C.; Paul, K. E.; Whitesides, G. M. *Adv. Mater*. **2001**, *13*, 604−607.
(18) Wu, M. H.; Paul, K. E.; Yang, J.; Whitesides, G. M. *Appl. Phys. Lett*. **2002**, *80*, 3500−3502.
(19) Spector, S. J.; Astolfi, D. K.; Doran, S. P.; Lyszczarz, T. M.; Raynolds, J. E. *J. Vac. Sci. Technol., B* **2001**, *19*, 2757−2760.
(20) Kristensen, R. T.; Beausang, J. F.; DePoy, D. M. *J. Appl. Phys*. **2004**, *95*, 4845−4851.
(21) Jensen, T. R.; Schatz, G. C.; Van Duyne, R. P. *J. Phys. Chem. B* **1999**, *103*, 2394−2401.
(22) Haes, A. J.; Van Duyne, R. P. *J. Am. Chem. Soc*. **2002**, *124*, 10596−10604.
(23) Puscasu, I.; Spencer, D.; Boreman, G. D. *Appl. Opt*. **2000**, *39*, 1570−1574.
(24) Byrne, D. M.; Brouns, A. J.; Case, F. C.; Tiberio, R. C.; Whitehead, B. L.; Wolf, E. D. *J. Vac. Sci. Technol., B* **1985**, *3*, 268−271.
(25) Gates, B. D.; Xu, Q.; Stewart, M.; Ryan, D.; Willson, C. G.; Whitesides, G. M. *Chem. Rev*. **2005**, *105*, 1171−1196.
(26) Gates, B. D.; Xu, Q. B.; Love, J. C.; Wolfe, D. B.; Whitesides, G. M. *Annu. Rev. Mater. Res*. **2004**, *34*, 339−372.
(27) Xia, Y.; Whitesides, G. M. *Angew. Chem., Int. Ed*. **1998**, *37*, 550−575.
(28) Bowden, N.; Terfort, A.; Carbeck, J.; Whitesides, G. M. *Science* **1997**, *276*, 233−235.

NL0713979